UNCLASSIFIED

AD NUMBER
AD233215
LIMITATION CHANGES
TO: **Approved for public release; distribution is unlimited.**
FROM: **Distribution authorized to DoD and DoD contractors only; Administrative/Operational Use; SEP 1959. Other requests shall be referred to Army Transportation Research and Engineering Command, Fort Eustis, VA.**
AUTHORITY
TRECOM ltr Jan 1975

THIS PAGE IS UNCLASSIFIED

DEI SUB NUMINE VIGET

VET TESTAMENTUM NOV TESTAMENTUM

PRINCETON UNIVERSITY

DEPARTMENT OF AERONAUTICAL ENGINEERING

716300

U. S. Army Transportation Research and Engineering Command
Fort Eustis, Virginia

Project Number: 9-38-01-000, TK902
Contract Number: DA44-177-TC-524

SOME QUALITATIVE CHARACTERISTICS

OF A

TWO-DIMENSIONAL PERIPHERAL JET

by

W. B. Nixon and T. E. Sweeney

Department of Aeronautical Engineering

Princeton University

Report No. 484 September, 1959

Approved by:

C. D. Perkins

C. D. Perkins, Chairman
Department of Aeronautical
Engineering, Princeton University

FOREWORD

The material presented in this report is the result of experiments conducted at Princeton University under the sponsorship of the U. S. Army, TRECOM. This work is part of the ALART program, phase 2 of which is directed toward basic studies of the ground effect phenomenon. This report is the first of a series covering the results of experimental and theoretical ground effect research performed at Princeton during the time period September 1958 through December 1959.

TABLE OF CONTENTS

SUMMARY

~~This report deals exclusively with~~ base pressure distributions of a 2 ~~two~~-dimensional peripheral jet model in simulated hovering flight is discussed. Flow patterns were ~~have been~~ deduced from these distributions and were ~~have been~~ verified with smoke studies. The standing vortex associated with this type of device is plotted as a function of altitude and angle of inclination, and the relationship between the vortex and static instability is shown for 3 ~~three~~ initial jet angles.

Also included is a brief discussion of the unsteady flow pattern generated at certain altitudes and initial jet angles. This flow is plotted and is shown to deteriorate, apparently, into a Karman street - possibly explaining the critical altitude reported by other investigators.

I. INTRODUCTION

The static studies reported herein were begun because of a lack of two-dimensional information in the rather sparse literature dealing with the peripheral jet in proximity to the ground. An understanding of the basic flows appeared desirable for furthering the state of knowledge in this field and for explaining, perhaps, some observations previously reported by other investigators.

These experiments were exploratory in nature, which explains why no attempt was made to systematically vary all parameters. Only those factors pertinent to a qualitative insight into some of the dominant characteristics of the flow contained within the peripheral jet were considered. No attempt has been made to extrapolate the results to the three-dimensional case, although observations in the course of subsequent three-dimensional experiments suggest applicability of the two-dimensional findings to this case.

II. DISCUSSION

A. Apparatus

The experimental apparatus used for this study is shown in the photograph and drawing of Figure 1. The blower provided pressure ratios as high as 1.1, although much of the experiment was performed at lower pressure ratios. This parameter was dictated by the capacity of the smoke generator, which, due to mixing of the jets with the more quiescent enclosed air, could provide visible smoke only at much lower jet velocities. Model configurations are shown in Figure 2. The model was made of wood; however, the nozzle blocks were of machined aluminum, carefully spaced and aligned to assure symmetry with regard to slot width and angle of blowing ($\theta_o = 0^o$).

B. Experiments

Since lift augmentation at constant mass flow was not of particular importance to these experiments, no attempt was made to maintain a constant slot velocity for the altitude range under study. Rather, a constant blower power setting was established, which permitted ΔP and mass flow variations much as they would occur in a free flight machine with a given air horsepower capability.

Manometer readings were recorded for several values of h/b and angles of inclination (α). These results are presented in Figures 3 and 4. Figure 3a shows the typical variations in base pressure with altitude for zero angle of inclination in the static condition. The very gentle wave shape of the pressure distribution at high h/b is observed to develop into rather pronounced peaks separated by a broad flat valley as h/b is reduced.

Such pressure distribution characteristics suggested the presence of a vortex, which was deduced to appear as shown in Figure 3b. Smoke studies confirmed the presence of the vortex and its behavior with altitude. It is interesting to note that the diameter of the vortex appears to be equal to the distance of the model from the ground plane. As this height is reduced, the vortex diameter becomes smaller, and the core of the vortex moves on a 45° path toward the slot in the manner shown in Figure 3b.

As indicated by the pressure distributions and as observed during the smoke studies, the vortex tends to maintain a constant circulation, since at the higher values of h/b, the vortex is large and slow, becoming faster as its size is reduced with decreasing altitude.

Figure 4a shows the base pressures for several values of α . It should be observed that the shape of these curves is such as to move the center of pressure toward the high end of the model, which, of course, indicates static instability. This characteristic appears to be associated with the vortex behavior as shown in Figure 4b. It should be noted that the two segments of a vortex, as shown in Figure 3b, are tangent to the base of the level model. However, with increasing angle of inclination, the vortex segment on the high end separates from the base of the model, thus permitting the higher center base pressures to influence this region. The vortex segment on the low end of the model, however, is flattened slightly by tilting the model, causing the vortex to attach to the base to a greater extent than in the zero angle of inclination case. This lack of symmetry of the vortex segments relative to the base of the model

seems to explain, at least in part, the characteristic pressure distributions for the tilted model. Another flow characteristic tending to produce the pressure distributions shown in Figure 4a is the spillage from the high end. This results in a portion of the air from the low slot passing beneath the base and ejecting from the high end. Thus, the two-dimensional model in proximity to the ground plane becomes an effective two-dimensional diffuser for this transverse flow.

Once again, looking at Figure 3, it can be easily seen that there is apparently some lack of symmetry in the flow for the $\alpha = 0^{\circ}$ case. This is probably due to slight asymmetries in the construction of the model. It is significant, however, that the asymmetric vortex behavior associated with tilted models was achieved regardless of direction of tilt (+ or $-\alpha$). This would seem to indicate that the qualitative flow pictures presented in Figure 4 are not the result of the almost unavoidable model asymmetries, but that they are inherently a function of the angle of tilt.

The next phase of this work utilized model configurations b and c. These differed from the original configuration by the addition of curved metal vanes attached in such a manner as to turn the peripheral jet inward, in one case 45°, and in the other 80°, from the vertical. The pressure ratio for these studies was approximately 1.04 and the height of the model above the ground plane was measured from the bottom of the vanes.

Base pressure distributions were graphically integrated and an average base pressure was obtained, which, being a function of both lift and augmentation ratio, was plotted versus h/b in Figure 5a. As shown in this Figure, there is a general improvement in performance at low altitudes as the initial jet angle is increased in the negative direction, as predicted by theory. More significant, however, is the change in "critical altitude," the altitude where there is an obvious discontinuity in the lift curve. Smoke was injected into the cavity and the observed characteristic flow patterns are presented in Figure 5b. The first diagram for each configuration is a low altitude, balanced condition, while the second and third diagrams represent conditions just before and after the discontinuity. For initial jet angles of $\theta_o = 0^o$ and $\theta_o = -45^o$, the flow pattern degenerates into what appears to be an oscillating Karman vortex street, while for $\theta_o = -80^o$, the jet sheet curves upward and attaches to the base of the model.

Considering now the relationship between initial jet angle and static instability, Figures 3 and 4 indicate that the vortex is the source of the unfavorable pressure distribution, while Figure 5 shows that turning the jet inward displaces the vortex toward the center of the base and, thus, tends to reduce its effect. To measure this effect, the model was set at different inclinations (α) with h/b equal to 0.18, and the pressure distributions for the three initial jet angles were plotted. The location of the center of pressure was obtained and its displacement from mid-span was plotted versus inclination, along with average pressure. The results are shown in Figures 6a and 6b. It is seen that turning the jet inward appreciably decreases the static instability in the hovering case while definitely improving performance.

III. CONCLUDING REMARKS

Although no conclusions, as such, will be drawn, it is apparent from the results discussed in the previous section that certain deductions are in order:

A. For the two-dimensional $\alpha = 0$ condition, the vortex has a pronounced effect on base pressures, and this effect is detrimental to performance. The locally reduced base pressures, due to the vortex, tend to diminish relative to the average base pressure as altitude is increased.

B. For the two-dimensional peripheral jet model inclined to the ground plane, the base pressure distribution is such as to displace the center of pressure toward the high end of model. This behavior is in general agreement with three-dimensional observations. The vortex pattern for the inclined two-dimensional model is such as to account, at least qualitatively for the nonsymmetrical pressure distribution. This is not to say that the vortex is completely responsible for the inherent instability of the configurations under study, since a transverse flow from the low end to the high end of the tilted model diffuses enroute, thereby contributing to the observed pressure distributions.

C. The discontinuity in the augmentation curve, reported by other investigators and observed in this study, appears to be related to the development of an apparent Karman vortex street. The initial jet angle, θ_o, appears to strongly influence the height at which the discontinuity occurs - the greater the negative value of θ, the lower the value of h/b that the Karman street occurs.

D. Blowing inward (initial jet angles negative) moves the vortex core toward the center of the base. For the cases tested, base pressures showed a substantial increase, and the effect of inclination of the base to the ground plane was not as pronounced as for the case of $\theta_0 = 0^\circ$, as far as the asymmetric pressure distribution is concerned. As a consequence the instability appears to be reduced for negative initial blowing angles.

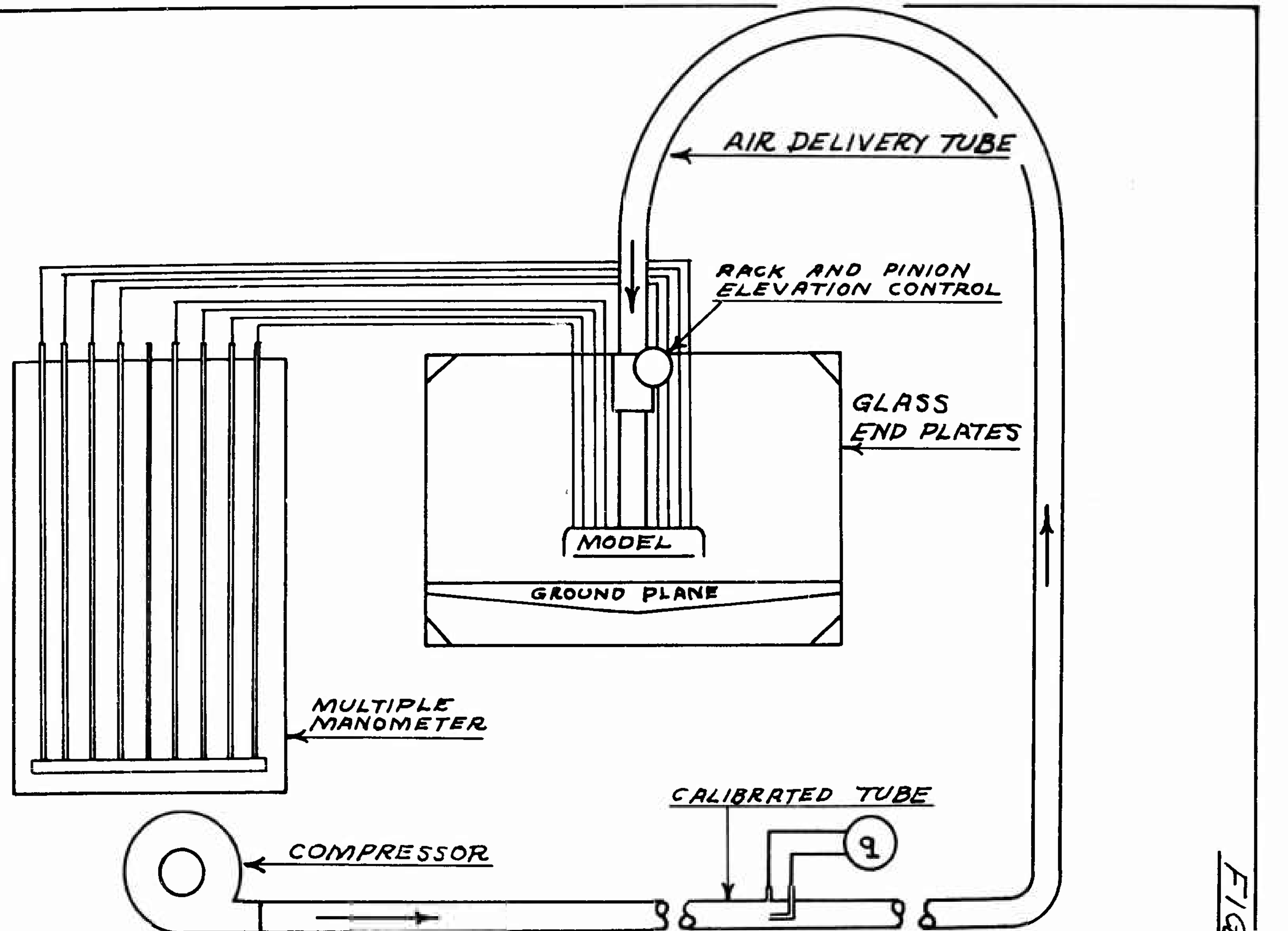

SCHEMATIC DIAGRAM OF EXPERIMENTAL SET UP

FIG. ~ 1

FIG.~2

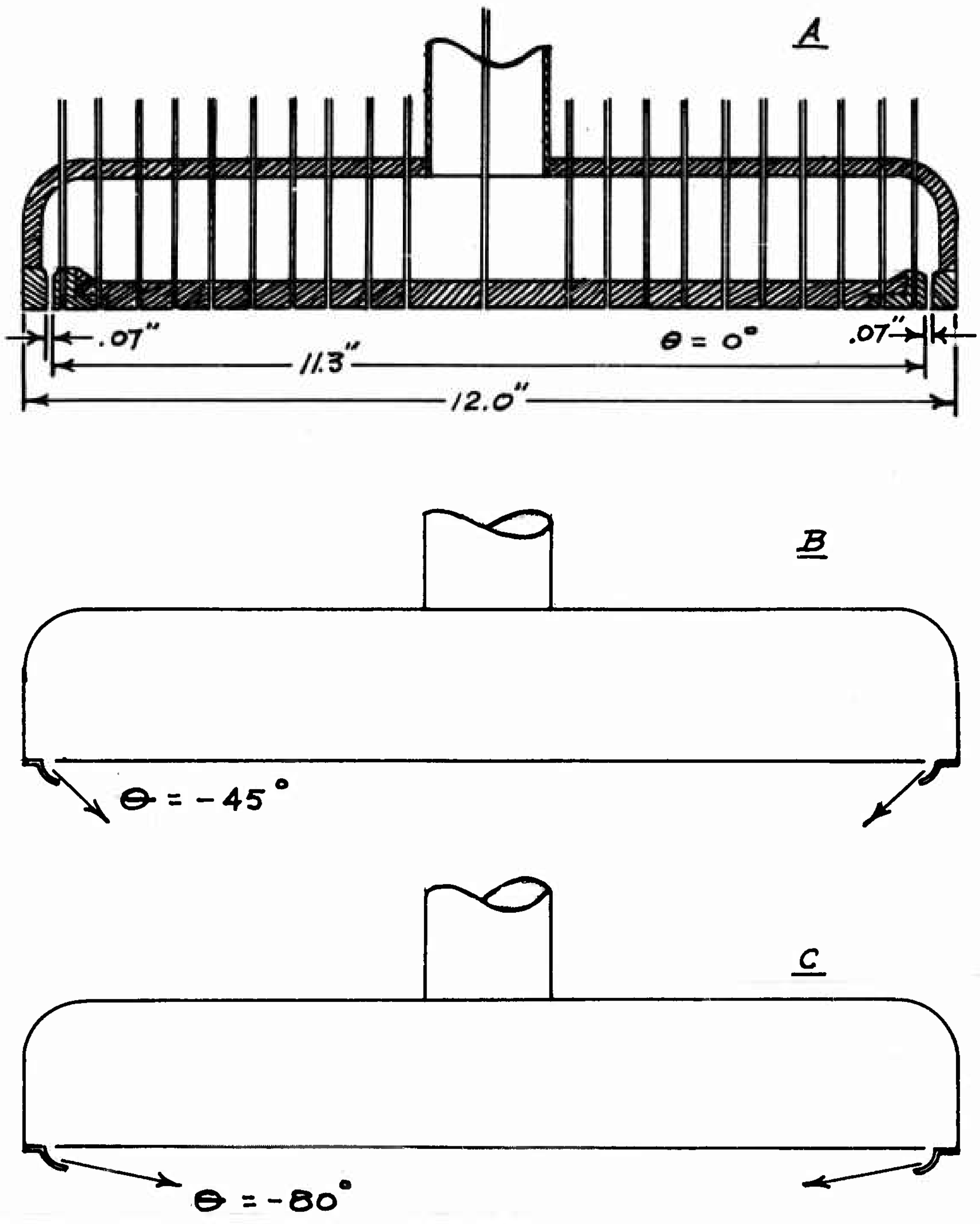

MODEL CONFIGURATIONS

TYPICAL BASE PRESSURE DISTRIBUTIONS FIG.~3a

$\alpha = 0°$, $\theta_o = 0°$

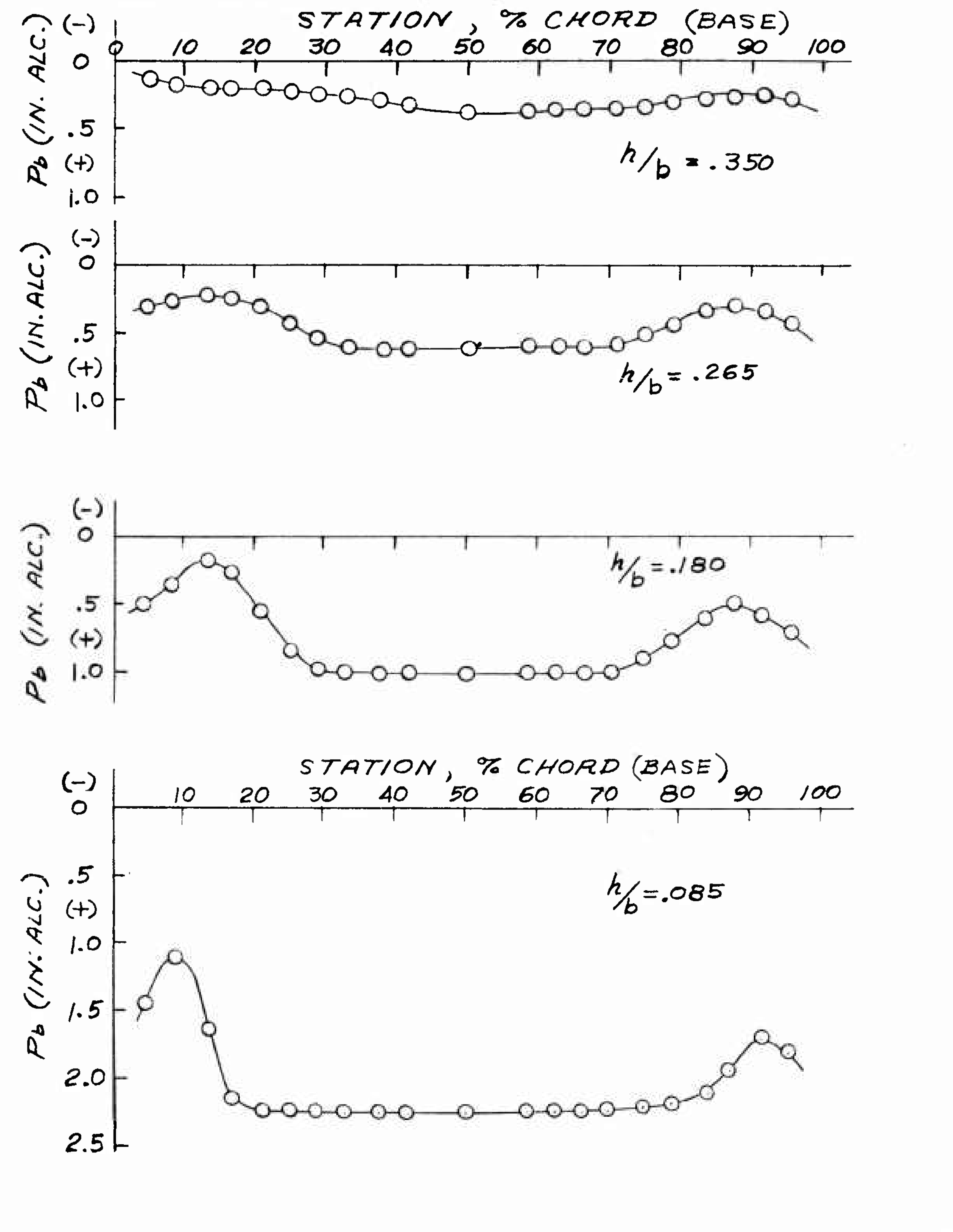

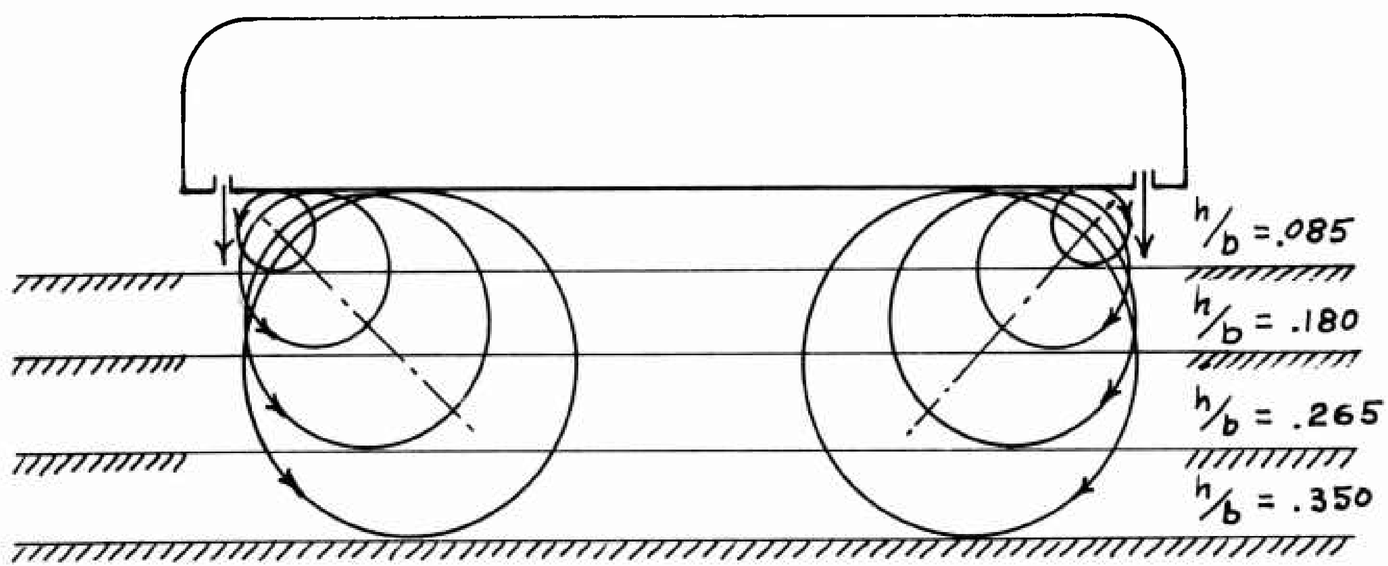

Typical Vortex Flow Pattern As A Function Of Altitude ($\alpha = 0°$, $\theta = 0°$)

Fig. 3b

TYPICAL PRESSURE DISTRIBUTION AS A FUNCTION OF α FIG. 4a

$h/b = 0.25$, $\theta_0 = 0°$

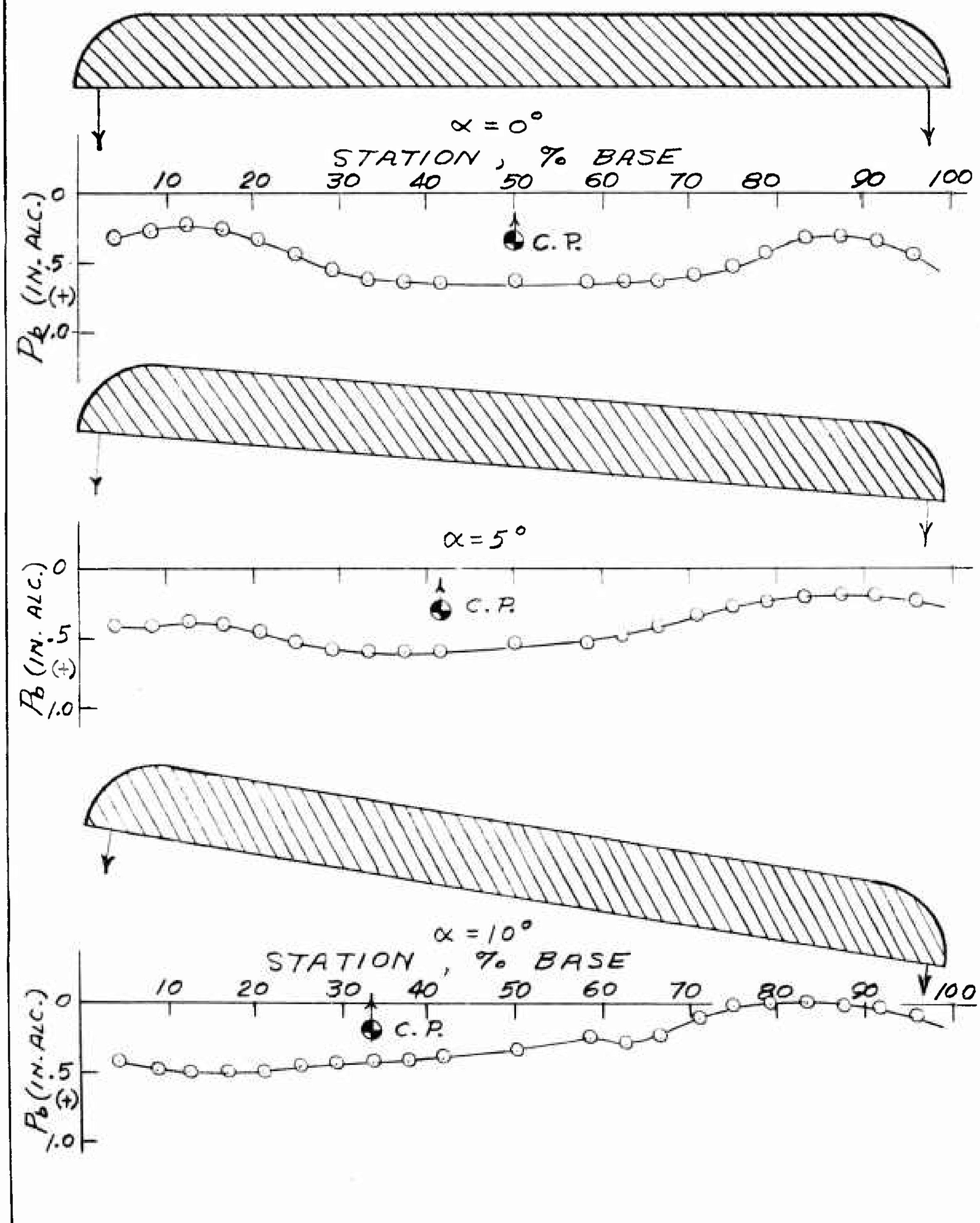

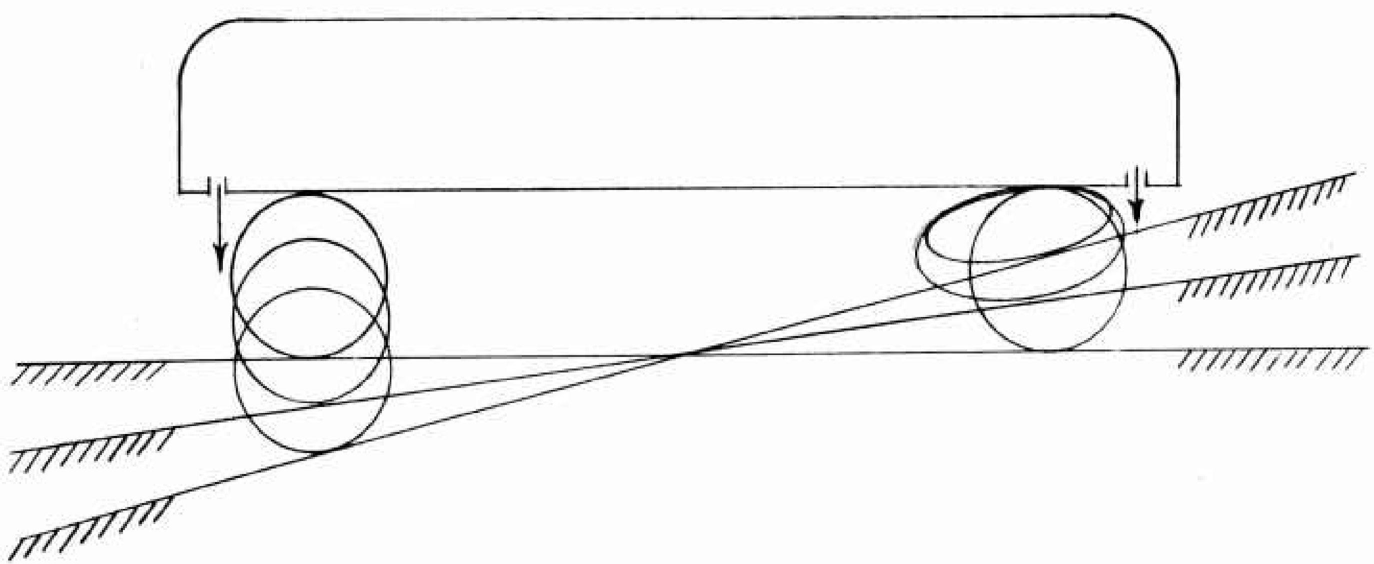

TYPICAL VORTEX FLOW PATTERN AS A FUNCTION OF α (h/b = CONST., $\theta_0 = 0°$)

FIG. 4-b

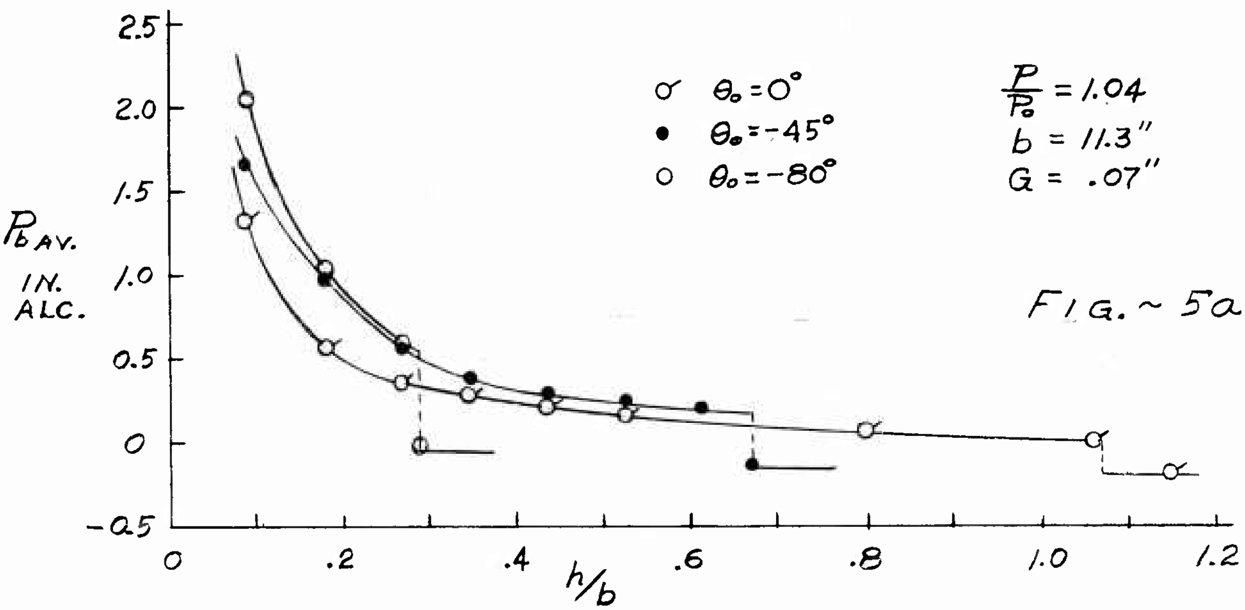

2.5
2.0
1.5
1.0
0.5
0
-0.5
$P_{b\,AV.}$
IN. ALC.
0
.2
.4
.6
.8
1.0
1.2
h/b
$\theta_o = 0°$
$\theta_o = -45°$
$\theta_o = -80°$
$\frac{P}{P_o} = 1.04$
$b = 11.3''$
$G = .07''$

FIG. ~ 5a

FIG. ~ 5b

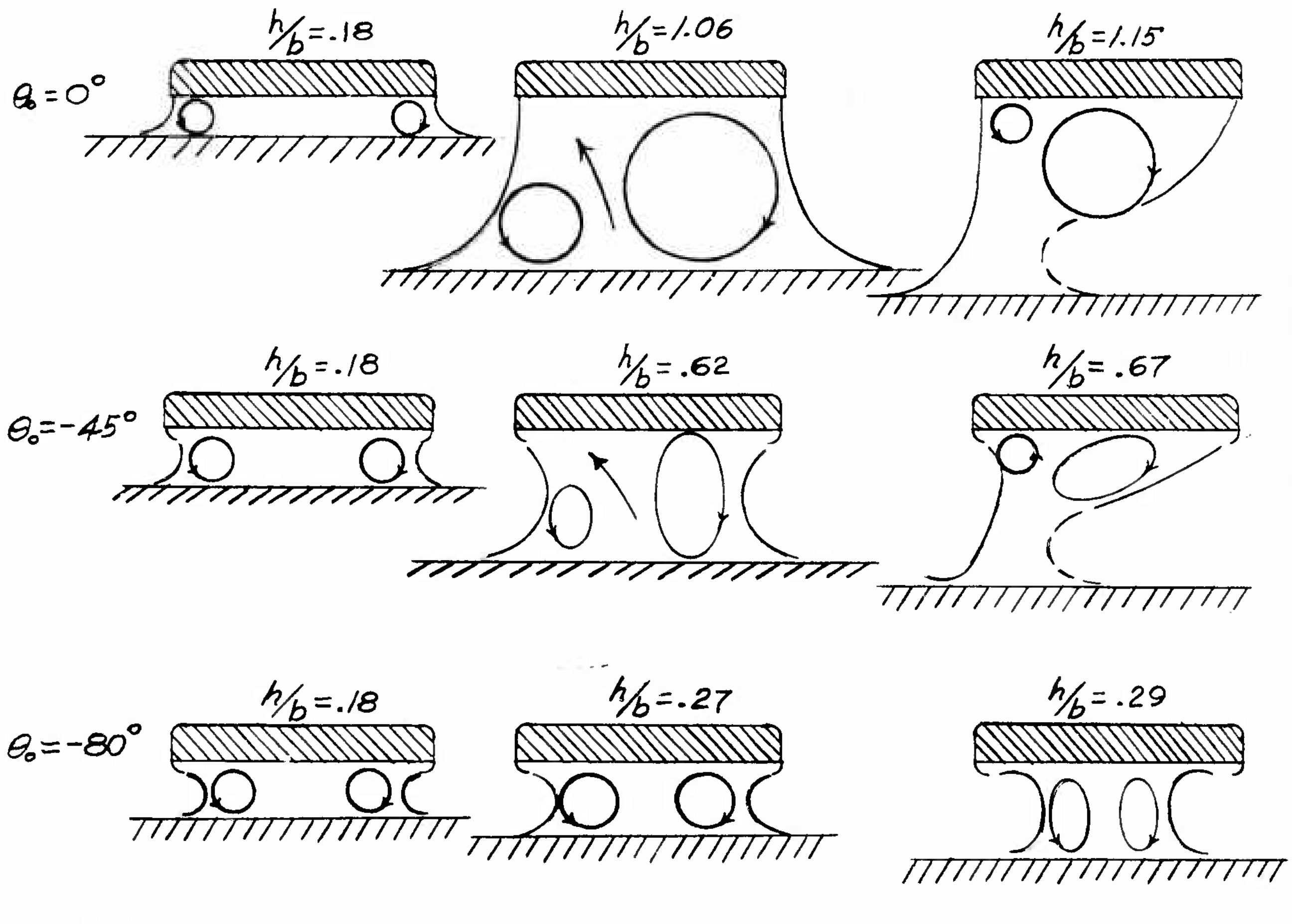

$\theta_o = 0°$
h/b = .18
h/b = 1.06
h/b = 1.15
$\theta_o = -45°$
h/b = .18
h/b = .62
h/b = .67
$\theta_o = -80°$
h/b = .18
h/b = .27
h/b = .29

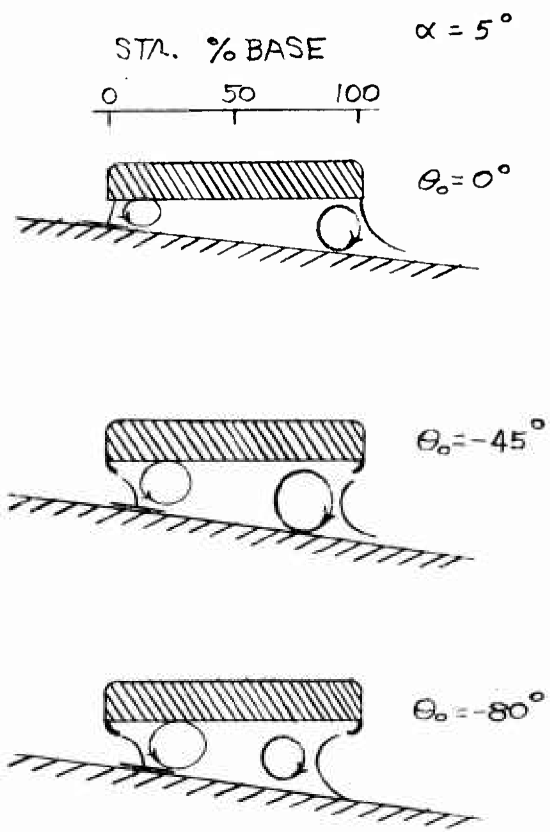

STA. % BASE
α = 5°
0
50
100
θ₀ = 0°
θ₀ = -45°
θ₀ = -80°

FIG. ~ 6a

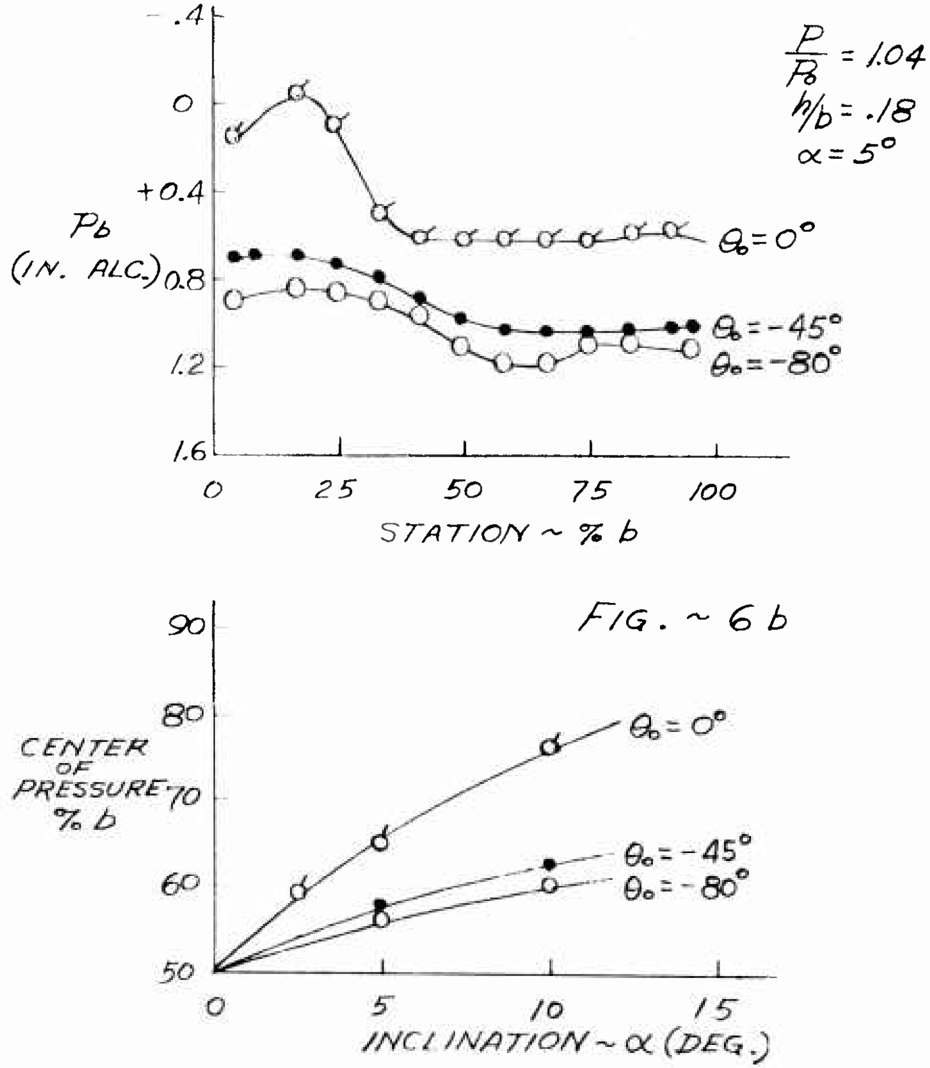

P/P₀ = 1.04
h/b = .18
α = 5°
Pb (IN. ALC.)
.4
0
+0.4
0.8
1.2
1.6
0
25
50
75
100
STATION ~ % b
θ₀ = 0°
θ₀ = -45°
θ₀ = -80°
CENTER OF PRESSURE % b
90
80
70
60
50
0
5
10
15
INCLINATION ~ α (DEG.)
θ₀ = 0°
θ₀ = -45°
θ₀ = -80°

FIG. ~ 6 b